JGR Biogeosciences

RESEARCH ARTICLE
10.1029/2023JG007640

Reoxidation of Reduced Peat Organic Matter by Dissolved Oxygen: Combined Laboratory Column-Breakthrough Experiments and In-Field Push-Pull Tests

Nikola Obradović[1], Prachi Joshi[1,2], Silvan Arn[1], Meret Aeppli[1,3], Martin H. Schroth[1], and Michael Sander[1]

[1]Department of Environmental Systems Science (D-USYS), Institute of Biogeochemistry and Pollutant Dynamics (IBP), Swiss Federal Institute of Technology (ETH) Zürich, Zürich, Switzerland, [2]Now at Geomicrobiology, Department of Geosciences, Eberhard Karls Universität Tübingen, Tübingen, Germany, [3]Now at Soil Biogeochemistry Laboratory, Environmental Engineering Institute, Swiss Federal Institute of Technology Lausanne (EPFL), Sion, Switzerland

Key Points:

- Peat particulate organic matter (POM) in the anoxic subsurface of three Swedish ombrotrophic bogs is present in reduced states
- Peat POM transfers 40–130 μmol e^- per g to dissolved oxygen with reaction times spanning from minutes to days
- POM acts as regenerable terminal electron acceptor in anaerobic respiration at oxic-anoxic interfaces in peat soils

Supporting Information:

Supporting Information may be found in the online version of this article.

Correspondence to:

M. H. Schroth and M. Sander,
martin.schroth@env.ethz.ch;
michael.sander@env.ethz.ch

Citation:

Obradović, N., Joshi, P., Arn, S., Aeppli, M., Schroth, M. H., & Sander, M. (2023). Reoxidation of reduced peat organic matter by dissolved oxygen: Combined laboratory column-breakthrough experiments and in-field push-pull tests. *Journal of Geophysical Research: Biogeosciences*, *128*, e2023JG007640. https://doi.org/10.1029/2023JG007640

Received 16 JUN 2023
Accepted 23 OCT 2023

Abstract Electron transfer to peat particulate organic matter (POM) as terminal electron acceptor (TEA) in anaerobic respiration has been hypothesized to lower methane emissions from peatlands by competitively suppressing methanogenesis and/or allowing for anaerobic oxidation of methane. We herein provide evidence for two critical aspects of this hypothesis: (a) peat POM is present in a reduced state in situ in the anoxic peat subsurface, and (b) reduced POM at the oxic-anoxic interface in peat soils can be oxidized by dissolved oxygen (DO), restoring its TEA capacity. We reacted reduced POM from three ombrotrophic bogs in Sweden with DO in soil-packed column-breakthrough experiments (CBEs), mimicking oxidation reactions at the oxic-anoxic interface. Breakthrough of DO was substantially retarded relative to the inert tracer bromide, consistent with DO reduction by POM. Control experiments confirmed abiotic DO reduction and excluded DO consumption through aerobic respiration. Modeling DO breakthrough revealed fast and slowly reacting POM moieties with reaction times spanning minutes to days. Complementary push-pull tests (PPTs) in the anoxic subsurface of one bog confirmed results from laboratory CBEs: lower recoveries of injected DO compared with bromide supported DO reduction by reduced POM. Rates of reduction of injected DO decreased with increasing number of injections, consistent with continuous oxidation of reduced POM. Electron-donating capacities of POM to DO in CBEs and PPTs were comparable at 40–130 μmol e^-/g dry POM. Our results substantiate that POM is a regenerable TEA at oxic-anoxic interfaces in peat soils and, thereby, may substantially lower CH_4 emissions from peatlands.

Plain Language Summary Northern peatland soils contain large amounts of carbon stored as peat particulate organic matter (POM). Understanding how microorganisms turn over this carbon is important because turnover can release not only carbon dioxide but also methane, a more potent warming gas. Recent literature proposes that microorganisms in oxygen-free parts of peat soils can turn over carbon substrate molecules by oxidation to carbon dioxide coupled to transferring electrons liberated in this process to POM. This newly proposed pathway is expected to substantially lower methane formation and emissions but relies on POM's ability to accept electrons. However, continuous electron transfer to POM in oxygen-free soil parts would eventually consume the capacity of POM to accept electrons, at which point methane formation would set in. In our work, we show that the electrons stored in POM under anoxic conditions can be transferred to dissolved oxygen (DO) which periodically enters the peat soils by various means. Reaction with DO thus restores POM's capacity to accept electrons in subsequent oxygen-free periods and thus its potential to suppress methane emissions. Our findings will help to better understand the role of POM in peatland carbon turnover to carbon dioxide and methane.

1. Introduction

Northern peatlands are a major global carbon pool, storing an estimated 500–1,055 Gt carbon, an amount that corresponds to as much as 30%–60% of the total global soil organic carbon stock (Christensen et al., 1997; Gorham, 1991; Hiederer & Köchy, 2011; Nichols & Peteet, 2019; Scharlemann et al., 2014; Z. C. Yu, 2012; Z. Yu et al., 2011). More than 98.5% of peatland carbon is stored in peat soils in the form of peat particulate organic matter (POM) (Gorham, 1991), the solid peat-forming material that results from incomplete decomposition of

vegetation litter. This carbon has accumulated since the last glaciation owing to carbon fixation by peat vegetation exceeding slow decomposition of the vegetation litter in the water-logged, nutrient-poor, low pH, and cold peat-soil environments typical for these ecosystems (Beer et al., 2008; Freeman et al., 2001; Scheffer et al., 2001). There is significant interest in understanding how carbon is turned over in northern peatlands, especially in the context of ongoing and expected future global warming (IPCC, 2022). Processes that control the formation and emission of the potent greenhouse gas methane (CH_4) are of particular interest: currently, northern peatlands account for an estimated 24%–33% of the annual CH_4 emissions from natural sources (Forster et al., 2007; IPCC, 2022; Lai, 2009; Salmon et al., 2022; Saunois et al., 2020).

Recent studies provided evidence for anaerobic respiration prevailing over methanogenesis in anoxic parts of peat soils even when pore waters contained only very low concentrations of the canonical inorganic terminal electron acceptors (TEA) (i.e., sulfate, nitrate, iron(III), and manganese(IV)) used for anaerobic respiration (Lindsay, 2016; Moore et al., 2005). These studies hypothesized that peat POM is an unrecognized TEA for anaerobic respiration (Bridgham et al., 2013; Broder et al., 2012; Gabriel et al., 2017; Keller & Takagi, 2013; Keller et al., 2009; Roden et al., 2010; Scott et al., 1998; Z.-G. Yu et al., 2016). This hypothesis builds on extensive past work, which demonstrated that dissolved organic matter (DOM) contains redox-active quinone groups that can reversibly accept electrons from anaerobic microbial respiration (Klüpfel et al., 2014; Lovley et al., 1996, 1998; Walpen et al., 2018a) to form hydroquinone groups.

Akin to anaerobic respiration to inorganic TEAs, respiration to POM could substantially lower methane concentrations in peat pore waters through two pathways. First, anaerobic respiration to POM is expected to be energetically more favorable than methanogenesis and thus is expected to competitively suppress the latter (Amaral & Knowles, 1994; Heitmann et al., 2007; Rissanen et al., 2017; Segers & Kengen, 1998; Ye et al., 2016). Results from peat soil incubations in the laboratory support this pathway (Efremenko et al., 2020; Gabriel et al., 2017; Gao et al., 2019; Keller & Takagi, 2013). Second, POM as TEA may allow for anaerobic oxidation of methane (AOM) formed within methanogenic zones in peat soils (Smemo & Yavitt, 2007, 2011). The AOM with a model dissolved quinone was recently demonstrated (Scheller et al., 2016), suggesting that this respiration pathway is possible also with electron-accepting quinone moieties in POM.

The use of POM as TEA in anaerobic respiration would stipulate that POM is present in a reduced state in anoxic parts of peat soils. At the same time, extensive use as TEA would lead to a depletion of the capacity of POM to accept additional electrons. Therefore, sustained anaerobic respiration to POM over longer time requires that the reduced POM undergoes periodic re-oxidation to regenerate its capacity to accept electrons. Such periodic re-oxidation is expected to occur by dissolved oxygen (DO) near oxic-anoxic interfaces in peat soils, and would render POM a sustainable, regenerable TEA. Intrusion of DO into the anoxic part of peat soils below the oxic-anoxic interface can occur by several means, including the percolation of rainwater or snowmelt (Blodau, 2002; Rydin & Jeglum, 2013; Stepniewski & Glinski, 1988), water-table drawdowns (Estop-Aragones et al., 2012; Gabriel et al., 2017; Gorecki et al., 2021), transfer through plant aerenchyma (Agethen et al., 2018), and through the release of photosynthetically produced DO from roots and sphagnum rhizoids (Björn et al., 2022). Cyclic DO reduction and re-oxidation of POM may thus favor anaerobic respiration over methanogenesis specifically in the upper part of peat soils, which receive high inputs of fresh labile carbon substrates (Yang et al., 2017). Moreover, POM at the redox interface may allow for anaerobic oxidation of CH_4 formed in methanogenic zones of peat soils below the oxic/anoxic interface. Quantifying the number of electrons donated from extensively reduced POM to DO would allow for estimating the number of electrons that POM accepted from anaerobic respiration.

We previously provided first evidence for POM being in a reduced state in the anoxic, water-saturated part of an ombrotrophic bog (Lungsmossen (LM), Värmland, Sweden) by demonstrating that this POM transferred electrons to DO that we injected into the peat subsurface (Walpen et al., 2018b). However, we used single DO injections, which resulted in fast and complete DO reduction in the peat subsurface and thus did not allow to quantify the total number of electrons that reduced POM donates to DO. In a follow-up laboratory batch-reactor study, we demonstrated that exposing reduced POM from anoxic parts of two bogs (i.e., LM and Björsmossen (BM)) to DO for 8 d resulted in substantial POM oxidation, as evidenced from much higher capacities of re-oxidized POM to accept electrons in a chemical reduction assay as compared to the non-re-oxidized POM in the same assay (Joshi et al., 2021). Measured electron-accepting capacities ranged from 180 ± 30 to 260 ± 30 μmol e^-/g dry peat for the reduced and DO-oxidized LM POM, and from 240 ± 30 to 330 ± 40 μmol e^-/g dry peat for the reduced and DO-oxidized BM POM. In the same study, we also showed reversible electron transfer to a reference POM

material over an electrochemical reduction and subsequent DO re-oxidation cycle. However, in our previous work we did not assess the transferability of results from POM oxidation experiments in laboratory batch reactors to POM oxidation in the field in situ. Furthermore, the past studies omitted information on the rates of electron transfer from POM to DO. This information is critical to assess the reaction times over which the capacities of POM to accept electrons are restored during recurring DO oxidation events in peat soils.

The goal of this work was to provide quantitative information on both rates and capacities of electron transfer from reduced POM to DO in peat soils from different ombrotrophic bogs, and to assess the transferability of results obtained in laboratory experiments to the in situ conditions in the field. To this end, we first determined rates and capacities of POM oxidation by DO in laboratory column-breakthrough experiments (CBEs) using columns packed anoxically with reduced peat soils collected in three ombrotrophic bogs. The DO reduction rates and extents were determined by fitting tracer and DO breakthrough curves using a solute transport—kinetic reaction model. We complemented these laboratory CBEs with in-field single-well injection-extraction tests (i.e., push-pull tests (PPTs)), in which we quantified the decreases in DO concentrations of oxic test solutions that we repeatedly injected into and retrieved from the anoxic peat soil below the oxic-anoxic interface. Collectively, this work quantifies rates and capacities of electron transfer from reduced POM to DO in different peatlands, thereby providing missing information on the regeneration dynamics of POM as TEA at the oxic-anoxic interface in peat soils.

2. Materials and Methods

2.1. Field Sites, Pore-Water and Peat-Soil Characterization

For our work we chose three ombrotrophic bogs in Värmland county, Sweden, that we had previously studied (Joshi et al., 2021; Walpen et al., 2016, 2018a, 2018b): LM (N 59°32.969′E 14°14.313′), BM (N 59°41.557′E 14°16.629′), and Storhultsmossen (SM, N 59°34.301′E 14°07.908′). The vegetation in these bogs is dominated by *Sphagnum* carpets and hummocks with few isolated trees (mostly *Pinus sylvestris*), as was previously described for bogs in this region (Almquist-Jacobson & Foster, 1995). The water tables were located at 5–15 cm below the peat surface. We chose ombrotrophic bogs because these systems contain comparatively low amounts of reduced inorganic species such as ferrous iron (Fe^{2+}) and sulfide (HS^-), which could contribute to DO reduction in our experiments. Pore waters collected from the three bogs ~25 cm below the water table contained Fe^{2+} concentrations ranging from 0 to 7 μM, and HS^- concentrations ranging from 2 to 13 μM (Text S1 in Supporting Information S1). The data for LM and SM are in good agreement with Fe^{2+} and HS^- concentrations we previously determined in pore waters of these two bogs (Walpen et al., 2016, 2018a). Moreover, the data for all three bogs strongly suggest that contributions of Fe^{2+} and HS^- to DO reduction were negligible given the much larger amount of DO reduced when reacted with reduced POM (see below). We characterized peat-soil samples by elemental and spectroscopic analyses, as detailed in the Text S2 and S3 in Supporting Information S1.

2.2. Column-Breakthrough Experiments

2.2.1. Peat-Soil Collection and Column Packing

To quantify rates and capacities of electron transfer from reduced POM to DO, we conducted a series of CBEs in water-saturated peat-soil packs. In each bog, we manually collected anoxic peat soil from a depth of 30–40 cm below the water table. Column packing for experiments conducted at our field laboratory was done directly in the field by submersing and filling columns anoxically with peat soil at the sampled depth. For CBEs conducted at the ETH laboratory (specifically identified below), columns were packed in an anoxic glovebox (atmosphere of 99.999% N_2, O_2 < 2.3 ppm) with peat soil brought to the laboratory in sealed glass jars. The jars were filled with peat soil anoxically in the field at the sampled depth. Upon retrieval to the peat surface, these jars were immediately closed air-tight with a lid to prevent oxygen intrusion, stored in a cooler and refrigerator, and then transported to our ETH laboratory. Further information is provided in Text S4 in Supporting Information S1.

2.2.2. Experimental Design

Our experimental design allowed for operation of up to three columns in parallel inside a refrigerator maintained at 10–13°C (Figure 1), which corresponded to the temperature at the redox interface of the peat soils determined in the months of June and July. Flow of aqueous test solutions through the vertically mounted columns (either small (86 mL void volume) or large (160 mL) FlashPure Empty Solid Loader, Büchi, Flawil, Switzerland) was in the upward direction at a constant volumetric flow rate (2.4 mL/min for small and 3.0 mL/min for large columns)

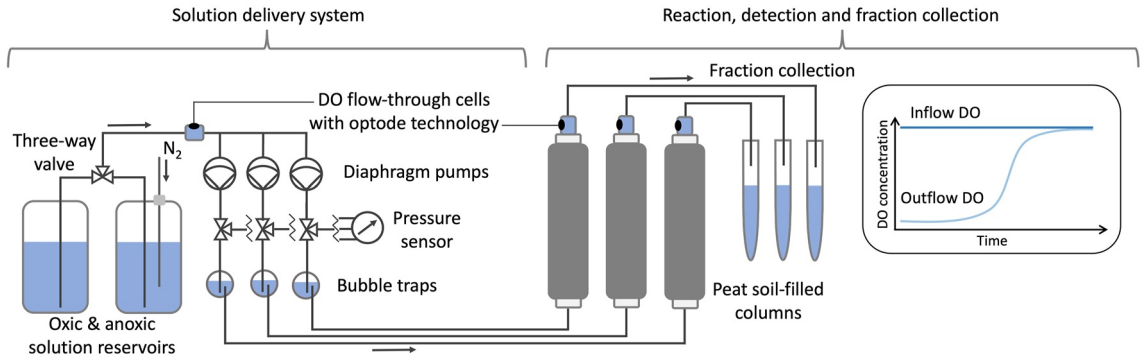

Figure 1. Experimental design for column-breakthrough experiments. Oxic or N_2-sparged (anoxic) test solutions were delivered using diaphragm pumps, with bubble-traps installed before the peat-soil-filled columns. Dissolved oxygen (DO) concentrations and temperatures in the inflow as well as each of the three columns' outflows were continuously measured using four O_2 flow-through cells with optode technology connected by fiber optics to a DO measurement system. Except for the DO measurement system, all equipment was housed inside a refrigerator maintained at 10–13°C.

using SIMDOS-02 and -10 diaphragm pumps (KNF Neuberger AG, Balterswil, Switzerland). To prevent gas bubbles from entering the columns with test solutions, we installed bubble traps before the column inlets. Back-pressure was monitored at the column inflow using a manometer (LEO 1, Keller, Winterthur, Switzerland) to allow for intervention in the rare case of column clogging. For tracer breakthrough analysis, the column outflow was manually collected in fractions (see below). Concentrations of DO and temperature in the inflow as well as each of the three columns' outflows were continuously measured using four O_2 flow-through cells with optode technology (PSt7and10 optodes, Pt-100 temperature sensors), which were connected by fiber optics to an OXY-4 trace measurement system (all from PreSens, Regensburg, Germany).

2.2.3. Characterization of Peat-Soil-Pack Physical Parameters

The internal pore volume (ipv) available to aqueous flow and the porosity of peat-soil packs in columns were determined for each CBE by first amending inflow solutions with the inert tracer bromide (Br^-) (i.e., tracer concentrations of 0.5 or 1.0 mM Br^-, prepared from NaBr, Sigma Aldrich, Schaffhausen, Switzerland), followed by determining Br^- breakthrough in the column outflow. Concentrations of Br^- in the collected outflow fractions (25 fractions per column, equivalent to a total of ∼2.5 pore volumes (PV; note that PV correspond to the cumulative solution volume delivered to the column, normalized to the ipv), collected during the first 125 min of each experiment) were quantified by ion chromatography for experiments conducted at ETH (Text S5 in Supporting Information S1), and electrical conductivity for CBEs conducted at our field laboratory. In the latter case, conductivity was used as a proxy for Br^- concentration given that ion chromatography was unavailable. We note that electrical conductivity in the column outflows increased not only because of Br^- breakthrough, but also because of an increase in aqueous H^+ concentrations (i.e., decrease in pH), which presumably resulted from the displacement of H^+ from POM by Na^+ from the tracer salt. We corrected for the H^+ contribution to conductivity after verifying the correction methodology, as detailed in Text S6 in Supporting Information S1. At the end of selected CBEs, we determined a second Br^- breakthrough (after flushing Br^- from peat-soil packs with anoxic, Br^--free solution) to confirm that column packing (and thus ipv and porosity) remained stable over the course of CBEs.

2.2.4. Quantification and Verification of Abiotic DO Reduction

To determine DO reduction by reduced POM in peat-soil packs (total of six columns from LM, and three columns each from BM and SM), we delivered test solutions containing DO (i.e., ∼90%–100% air-saturated) and formaldehyde (1% w/w, Fisher Chemical, Reinach, Switzerland) in addition to Br^- to the large columns. Variations in solution composition for selected CBEs are described below. Formaldehyde served as microbial inhibitor (Tuominen et al., 1994) to ensure that abiotic electron transfer from reduced POM to DO dominated over DO consumption through aerobic microbial respiration.

For CBEs in our field laboratory, test solutions delivered to the columns were prepared from water collected from an open-water pool in LM. Before delivery, these pool waters were consecutively filtered through 90, 60, and 15 µm filters (Swagelok, Arbor Fluidtec, Wohlen, Switzerland). Test solutions for CBEs at the ETH laboratory were prepared from deionized water (Milli-Q IQ 7000, Merck, Darmstadt, Germany). During CBEs, a minimum of 32 PV of test solution was pumped through each column. The cumulative amount of DO reduced during CBEs

was quantified as the difference in column inflow and outflow DO concentrations integrated over the pumped test-solution volumes, accounting for the dead volumes before and after the peat-soil packs. In some CBEs (peat-soil packs from BM), following 24 hr of continuous delivery of test solution, we temporarily halted flow for 6 hr, followed by returning to the initial flow rate. This experimental variation served to increase DO residence time in the columns and thereby test for slow DO reduction by reduced POM.

We performed two additional variants of CBEs (in small columns) to corroborate that observed DO consumption in peat-soil packs was indeed abiotic. In the first variant, which was conducted at the ETH laboratory, we delivered anoxic formaldehyde solution (1% w/w) for 24 hr to the peat-soil packs (total of two from LM) prior to conducting CBEs with oxic test solutions. In this variant, we maintained a constant volumetric flow rate of 2.4 mL/min over the course of the entire experiment. In the second variant, which we conducted at our field laboratory (total of three peat-soil packs from LM, three from BM, and three from SM), we alternated delivery of DO-containing test solutions (oxic, see above) and anoxic test solutions. These anoxic test solutions were separately prepared from LM pool water by vigorous N_2 sparging. These anoxic solutions were amended with Br^-, but not with formaldehyde (as it would have been removed from the solutions during N_2 sparging). Once the first DO breakthrough was close to completion, we switched to pumping anoxic test solution through the columns until DO concentrations reached a minimum. This sequence was repeated once while maintaining a constant flow rate (2.4 mL/min) throughout these CBEs.

After termination of each CBE, the peat soil was removed from the column, flushed with deionized water, and dried at 50°C for 10 days for gravimetric determination of POM dry weight. The latter was used to normalize the amounts of DO reduced and hence to calculate POM-mass normalized electron transfer capacities from reduced POM to DO that can be compared across the different CBEs run with different POM masses.

2.2.5. Modeling Tracer and DO Breakthrough Curves

For each CBE we modeled Br^- and DO breakthrough in the column outflow using the Aquasim 2.0 software package (Reichert, 1994, 1998). Assuming one-dimensional steady-state water flow and advective-dispersive solute transport with reaction, the governing equation is:

$$\frac{\partial C}{\partial t} = D\frac{\partial^2 C}{\partial x^2} - \frac{Q}{A \cdot \theta_{\text{eff}}}\frac{\partial C}{\partial x} - r \tag{1}$$

where C (μmol L^{-1}) is aqueous solute concentration of either Br^- or DO, t (hr) is time, D (cm^2/hr) is the hydrodynamic dispersion coefficient, x (cm) is distance along the column length, Q (cm^3/hr) is volumetric flow rate, A (cm^2) is column cross-sectional area of the column interior, θ_{eff} (–) is the effective porosity of the peat-soil pack, and r (μmol (L h)) is a reaction term (see below) accounting for DO reduction by reduced POM.

We first fitted Equation 1 to Br^- breakthrough data with r set to zero to obtain best-fit values for D and θ_{eff} for each peat-soil pack. These values were subsequently used for modeling DO transport and reaction in respective CBEs. Two reaction models for DO reaction were employed, featuring either single ($n = 1$) or dual (fast and slow, $n = 2$) first-order-type kinetics:

$$r = \frac{\partial C_{O_2}}{\partial t} = \sum_{i=1}^{n} k_i C_{O_2}\left(1 - \frac{RM_i}{RM_{max,i}}\right) \tag{2}$$

where C_{O_2} (μmol/L) is the DO concentration, k_i (1/hr) is the rate constant of DO reduction by reduced POM moieties with kinetic i, RM_i (μmol/g) is the cumulative calculated number of POM moieties of kinetic i that have already reacted with DO and thus went from a reduced to an oxidized state, and $RM_{max,i}$ (μmol/g) is the maximum number of reduced POM moieties of kinetic i that can react with DO. By substituting Equation 2 in Equation 1 and fitting the latter to DO breakthrough data, we obtained best-fit values for k_i and $RM_{max,i}$. All best fits were obtained by minimizing χ^2 values between modeled and measured data using the secant algorithm built into Aquasim (Ralston & Jennrich, 1978).

2.3. Push-Pull Tests

2.3.1. Experimental PPT Design and Procedures

To determine the kinetics and extents of DO reaction with reduced POM directly in the field, we conducted PPTs in the LM peat soil at six locations (LM1–6). At these locations we inserted custom-built drive-point samplers into the peat soil to a depth of 30 cm. Each sampler consisted of a hollow stainless-steel tube (50 cm length,

3 mm i.d.) fitted with a perforated head with stainless steel screen (90 μm pore size) to facilitate manual fluid injection/extraction during PPTs using an air-tight plastic syringe attached to the sampler top.

Over a period of 12 consecutive days, we conducted 33 PPTs in each of LM1–3 and 34 PPTs in each of LM4–6. Each PPT included the following steps: (a) withdrawal of 350–450 mL pore water from the peat soil through the sampler into an open 2 L glass bottle, (b) oxygenating the collected pore water to obtain the DO-containing test solution (achieved by capping the 2 L bottle and thorough shaking), (c) injection of 300 mL of DO-containing test solution through the sampler into the peat soil, followed by (d) a rest period (no withdrawal) ranging from 1.5 to 23 hr to allow for prolonged reaction of DO with POM, and finally (e) extraction of 450 mL of solution (15 parcels of 30 mL each) that contained a mix of the injected test solution with background pore water from the same location in the peat soil. Extracting a volume 50% larger than the injected volume served to retrieve most of the injected solution and, thereby, minimize the amount of potentially unreacted DO left behind in the subsurface after each PPT. In selected PPTs with rest periods of 1.5 and 15.3 hr, we added Br^- (2 mM Br^- final concentration, prepared from NaBr) as inert tracer to test solutions to quantify their recovery in extracted solutions. In PPTs with rest periods >5 hr we added formaldehyde (1% by vol.) to test solutions as a microbial inhibitor (Tuominen et al., 1994) to ensure that there was no DO consumption by aerobic microbial respiration. Details for all PPTs are provided in Text S7 in Supporting Information S1.

To measure DO concentrations and temperatures of injected and retrieved solutions during PPTs, an O_2 flow-through cell was installed at the top of each sampler, connected by fiber optics to an Oxy1-ST analyzer (see above for details on products) coupled to a laptop computer. Water samples for Br^- analysis were collected from the injected test solution as well as from each extraction parcel, stored in plastic vials and transported to ETH, where they were analyzed by ion chromatography (Text S5 in Supporting Information S1). Details on the mathematical PPT analysis are provided in Text S8 in Supporting Information S1.

2.4. Estimation of Electron Donating Capacity of Reduced POM

We quantified the number of electrons transferred from reduced POM to DO based on measured abiotic DO reduction during CBEs and PPTs and assuming that each mol of DO (i.e., O_2) consumed was reduced by 4 mol e^- from reduced POM (i.e., complete reduction of O_2 to H_2O). We normalized this number of transferred electrons to peat-soil dry mass. The electron donating capacity of a unit mass of reduced POM (EDC, in μmol e^-/g) was then calculated as:

$$\mathrm{EDC} = \frac{4 \times n_{O_2}}{m_{\mathrm{POM}}} \tag{3}$$

where n_{O_2} (μmol) is the amount of DO reduced, and m_{POM} (g) is either the dry mass of peat-soil packs used in CBEs (Text S4 in Supporting Information S1) or the estimated dry mass of peat soil that was exposed to test solutions during PPTs (Text S9 in Supporting Information S1).

For CBEs, we operationally defined EDC as the amount of DO reduced over a total of 32 PV. Beyond 32 PV, reaction of DO with POM was very slow and not readily experimentally accessible. For PPTs, we converted the total amount of DO reduced to EDC by considering the measured peat soil porosities at both site clusters LM1-3 and LM4-6 to calculate the dry mass of POM in contact with the injected solutions (Text S9 in Supporting Information S1).

3. Results and Discussion

3.1. Column-Breakthrough Experiments (CBEs)

3.1.1. Reproducibility and Stability of Column Packing

The column packing was reproducible across CBEs, as shown by consistent effective porosities (i.e., ratio of PV to column void volume) between experiments (Table 1). Furthermore, the column packings were stable over the course of CBEs, as demonstrated in selected experiments by good agreement between a second tracer BTC collected at the end of the experiment and the tracer BTC collected at the onset of the experiment (Figure 2a). The effective porosity showed only a minor increase of 3.4 ± 0.8% (average ± standard deviation of six replicates (n = 6)) from the first to the second tracer BTCs, implying negligible compaction of peat-soil packing

Table 1
Average Peat Dry Masses (m_{POM}), Internal Pore Volumes (ipv), and Effective Porosities (θ_{eff}) of Columns Packed With Peat Soil From Lungsmossen (LM), Björsmossen (BM), and Storhultsmossen (SM)

Bog	Column type	Number of individual columns (n)	m_{POM} (g)	ipv (mL)	θ_{eff} (%)
LM	Large	6	17.4 ± 2.0	130 ± 5	81 ± 3
BM	Large	3	10.1 ± 1.5	140 ± 10	89 ± 6
SM	Large	3	12.9 ± 1.3	126 ± 5	78 ± 3
LM	Small	3	8.1 ± 0.8	76 ± 1	88 ± 1
BM	Small	3	7.5 ± 0.5	75 ± 3	87 ± 1
SM	Small	3	8.1 ± 0.4	73 ± 5	85 ± 1

Note. Large and small columns had void volumes of 160 and 86 mL, respectively.

inside the columns during the experiments. Packing the columns with peat soil from the three ombrotrophic bogs resulted in comparable effective porosities (Table 1). At the same time, for both small and large columns, dry peat masses in the columns showed higher variations between the three peat soils. We therefore normalized all DO reduction data (see below) to the dry mass of peat soil in the respective column. Furthermore, we normalized the total delivered solution volume to the PV of a given column. These normalizations allowed for comparison of BTCs between individual column experiments.

3.1.2. Abiotic Oxygen Consumption

Figure 2b shows the DO breakthrough from a representative CBE. The DO inflow concentrations were constant over the course of the experiment at around 280 µmol O_2/L (corresponding to 87% air saturation at an average temperature of 12.4°C and pressure of 984 mbar). The inflow DO concentration showed slight oscillations that resulted from small measurement artifacts due to small temperature fluctuations in the refrigerator that affected the sensor response (12.4 ± 0.6°C during 36 PV). The non-zero DO outflow concentrations at the onset of the experiment likely reflected oxygen that had diffused into the tubing connecting the column outlet with the DO flowthrough sensor. These DO concentrations readily decreased to a minimum within less than one PV of delivering DO saturated solutions to the column inlets, confirming that pore water inside the column was indeed anoxic in the beginning of the experiment. Beyond one PV, the outflow DO concentrations started to increase, indicating the onset of DO breakthrough.

The DO BTC was shifted to much higher PV as compared with that of the tracer bromide (comparison of Figures 2b and 2a). Also, as compared with the close-to-symmetric and sigmoidal tracer BTC, the DO BTC had a different shape: DO outflow concentrations increased in a sigmoidal manner only up to approximately 8 PV, after which DO outflow concentrations increased more gradually and only asymptotically approached the inflow DO concentration at high PV (Figure 2b). This finding implies that DO reacted in the peat-soil pack with varying kinetics: faster reaction kinetics governed the initial phase of the breakthrough, followed by a second phase until the end of the experiment with slower reaction kinetics. The distribution in reaction kinetics was also apparent from the cumulative amounts of DO reduced plotted versus delivered PV (Figure 2c): the amounts of reduced DO increased almost linearly with PV in the beginning of the experiment but then continuously decreased as the experiment progressed.

We conducted two types of control experiments to verify that decreases in DO concentrations in the columns were not caused by aerobic microbial respiration but instead by abiotic electron transfer from reduced POM to DO. The first type served to exclude the possibility that there was a time delay in the inhibition of aerobically respiring microorganisms by the microbial inhibitor formaldehyde present in the inflow solutions. Such delayed inhibition could, in principle, have caused the slow continuous DO consumption in CBEs. In LM peat-soil packs, we first delivered an anoxic formaldehyde solution for 35 PV (approx. 24 hr) to precondition the peat-soil pack to the inhibitor and to allow for sufficient time to inhibit microbial activity prior to introducing DO. As expected, DO concentrations in both the inflow and outflow were very low over this period (i.e., approximately 6 and 5 µmol/L in the in- and outflow, respectively) (Figure 3a). We subsequently delivered oxic test solutions. As observed previously in columns without formaldehyde pre-conditioning (Figures 2a and 2b), DO breakthrough was delayed relative to bromide (Br^- not shown in Figure 3a). Furthermore, even with formaldehyde pre-conditioning of the columns, DO concentrations in the column outflow only asymptotically approached DO inflow concentrations. The slightly faster initial increase in DO outflow concentrations as compared with experiments in which we did not precondition the columns with formaldehyde (Figure 2b) may reflect partial oxidation of fast-reacting reduced POM during the anoxic preconditioning: the solutions contained very low but measurable DO concentrations (see above). More importantly, however, the DO breakthrough curve was still retarded relative to the tracer and showed slow and prolonged DO reduction despite extensive formaldehyde preconditioning, excluding the possibility that these BTC features were caused by delayed microbial inhibition.

The second type of control experiment was performed with peat-soil packs from all three peats, LM, BM, and SM. We performed a first DO breakthrough as described above, but subsequently extended the experiment by delivering anoxic, oxic, and anoxic solutions in an alternating manner to the columns, with all oxic solutions containing

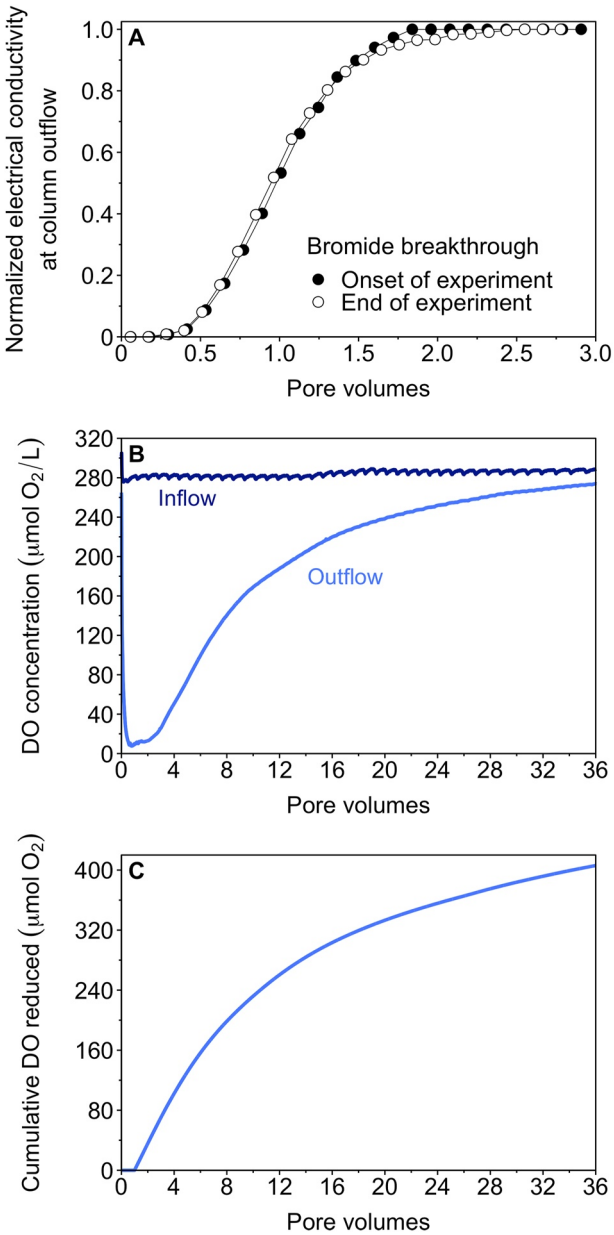

Figure 2. Exemplary breakthrough curves (BTCs) from a column-breakthrough experiment with a Lungsmossen (LM) peat-soil pack: (a) Tracer bromide BTCs expressed as normalized conductivity versus solution volume delivered to the column, expressed in pore volume equivalents, either at the onset or the end (i.e., at 24 hr) of the experiment. Bromide concentrations were measured in 25 discrete column-outflow volumes collected (symbols; lines serve to guide the eye); (b) The column inflow dissolved oxygen (DO) concentration profile (dark blue) and the column outflow DO concentration profile (light blue), both continuously measured; (c) The cumulative amount of DO reduced over the course of the breakthrough experiment shown in panel (b) The pore volumes correspond to the cumulative solution volume delivered to the column and normalized to the column-specific internal pore volume. The latter was determined for each packed column from a tracer breakthrough experiment.

formaldehyde (Figure 3b, shown for a representative experiment with LM peat-soil). The first DO breakthrough curves had similar shapes as the exemplary DO BTC shown in Figure 2b. Subsequent delivery of anoxic solutions to the column resulted in rapid decreases in DO concentrations in the column outflows, as expected. Importantly, when re-delivering DO-containing solutions, the second DO breakthrough occurred much more rapidly (i.e., within only a few PV) than in the first DO breakthrough. For instance, the amount of DO reduced in the column during the first 6 PV (i.e., approx. 3 hr) of delivering DO solutions was fivefold smaller in the second than first DO breakthrough. Decreased DO reduction in the second breakthrough strongly supports that the delay in the first DO breakthrough resulted from reaction of DO with reduced moieties in POM: oxidation of these moieties in the first DO breakthrough resulted in fewer moieties left to react during the second DO breakthrough. Consistently, Figure 3b shows that DO outflow concentrations in the second DO breakthrough rapidly increased to approximately the same values that were measured at the end of the first DO breakthrough when we switched from delivering oxic to anoxic solutions. This finding supports that DO reduction at the onset of the second DO breakthrough involved reaction with the same POM moieties that were left to react at the end of the first DO breakthrough. The final delivery of anoxic solutions again rapidly lowered DO in the column outflow, as expected. The results from this second type of control experiment rule out that DO in the columns was consumed by aerobic respiration, which would have continued (and possibly would have increased if aerobic microorganisms had replicated) during repeated delivery of DO.

Reduction of DO must have resulted from reaction with POM and not DOM for two reasons. First, while the packed peat columns likely contained reduced DOM at the onset of the experiments, this DOM was flushed out of the columns within a few PV of solution delivery and thus cannot explain the experimentally observed prolonged DO reduction over many PV. Also, the oxic solutions delivered to the columns contained oxidized DOM that cannot have reduced DO in the columns. Second, the total number of electrons transferred to DO (see below) by far exceeds the number of electrons that could be transferred to DO by DOM given the comparatively low DOM concentration in the column porewater and based on its previously reported redox capacities (even if DOM was present in a reduced state) (Walpen et al., 2018a).

3.1.3. DO Reduction by Peat Soil From Different Peatlands

We conducted a series of CBEs with peat-soil packs from LM, SM, and BM. While DO BTCs in SM and BM featured similar shapes to the ones of LM discussed above, the delay in DO breakthrough—and thus the amount of DO reduced—increased in the order of SM < LM < BM. This trend is particularly apparent from cumulative DO reduction up to 32 PV averaged over all CBEs of a given peatland ($n = 3$ for SM and BM, $n = 6$ for LM) (Figure 4): the total amount of DO reduced in BM and LM was approximately three- and twofold higher than in SM (see Text S4 and S10 in Supporting Information S1). The curves also highlight that amounts of DO reduced by peat soil from a given peatland are variable, with standard deviations being depicted as shaded areas: at 32 PV, the relative standard deviations in DO reduced were 17% for LM, 23% for BM, and 21% for SM. The differences in DO reduced between peat soils as well as the variations in DO reduced between soils from one bog most likely reflected differences in the source of POM as well as in its decomposition degree (Text S3 in Supporting Information S1). However, the variations in amounts of DO reduced among soil material from one peatland were smaller than variations between peat soils from different peatlands.

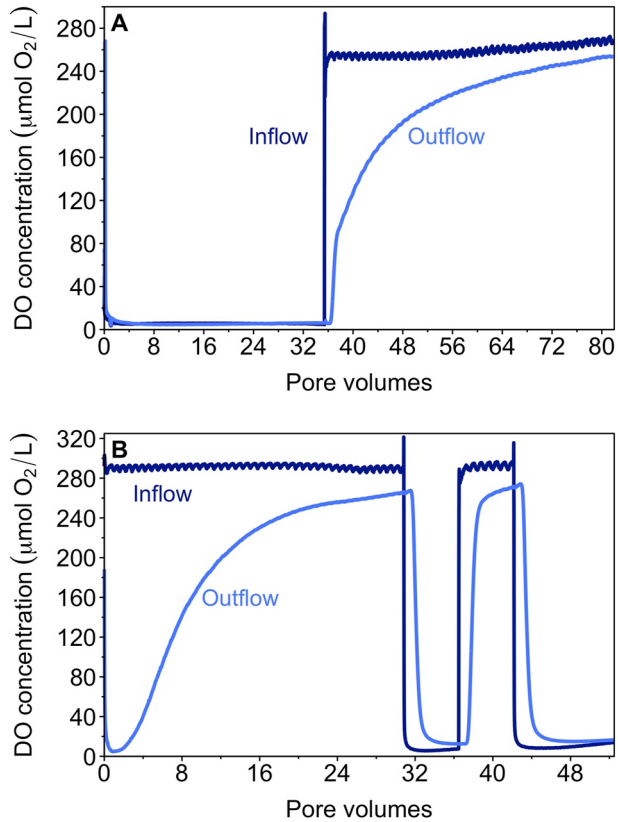

Figure 3. Exemplary results from two types of control experiments conducted to substantiate reduction of dissolved oxygen (DO) by peat particulate organic matter, each performed with peat-soil packs from Lungsmossen (LM). (a) Column in- and outflow DO concentrations during the initial delivery of anoxic, formaldehyde-containing solution to the column (first 35 pore volumes) and subsequent delivery of oxic solution; (b) Changes in column in- and outflow DO concentrations during an oxic-anoxic-oxic-anoxic cycling experiment. The pore volumes correspond to the cumulative solution volume delivered to the column and normalized to the column-specific internal pore volume. The latter was determined for each packed column from a tracer breakthrough experiment.

Figure 4 shows approximately linear increases in cumulative DO reduced over the initial few PV, followed by flattening of the curves (i.e., a continuous decrease in the amount of DO reduced per PV): of the total DO reduced over 32 PV approximately 50% reacted over the initial 8 PV for LM and BM and over 4 PV for SM. Therefore, the reaction of DO with POM for all peat soils showed varying kinetics.

Slow reaction kinetics between a fraction of reduced moieties in POM and DO were supported by selected CBEs in which we interrupted the flow of water in the columns after about 24 hr of delivery (approx. 32 PV, at which point the DO reduction was in the slow kinetic regime) for 6 hr (a time that corresponded to approximately 8 PV, if we had continued to deliver the solution at the used flow rates). The flow interruption increased the residence time of DO in the columns and therefore allowed for DO reduction also by slowly reacting, reduced POM moieties. Such slow reactions indeed occurred during the stopped flow, as was apparent from substantial drops in the DO outflow concentrations immediately after restarting the flow of water through the columns (Text S11 in Supporting Information S1). Following this initial drop, the DO outflow concentrations increased rapidly back to the concentrations measured prior to the flow interruption. The amount of DO reduced during the flow interruption was in good agreement with the amount of DO reduced during the same number of PV immediately prior to the flow interruption (calculated as DO consumption in the last PV prior to the flow interruption multiplied by 8).

3.1.4. Kinetic Modeling of DO Reduction

We modeled the DO BTCs using Equations 1 and 2, with either single or dual first-order type kinetics for the reduction of DO by reduced POM. For modeling, we set the DO concentration in the column outflow during the first PV (approx. 45 min) to zero. This correction was justified given that DO concentrations measured in

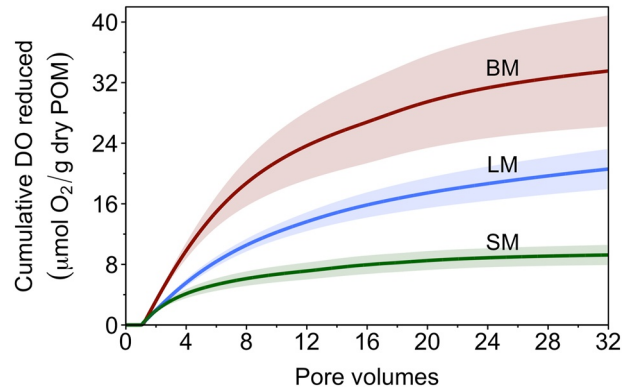

Figure 4. The averaged cumulative amounts of dissolved oxygen reduced in column-breakthrough experiments with peat soils from Lungsmossen (LM; $n = 6$), Björsmossen (BM; $n = 3$), and Storhultsmossen (SM; $n = 3$), where n is the number of columns packed with peat soil from the respective ombrotrophic bog. The amounts were normalized to dry mass of peat material in each peat-soil pack. The lines and shaded areas represent the averages and standard deviations, respectively. The pore volumes correspond to the cumulative solution volume delivered to the column and normalized to the column-specific internal pore volume. The latter was determined for each packed column from a tracer breakthrough experiment.

the first PV were very small and likely resulted from oxygen that had diffused into solution through the tubes that connected the column outlets to the oxygen sensors, as discussed above. Exemplary results of model fits to DO BTCs in LM peat-soil packs are shown in Figure 5. Fits with single-reaction kinetics failed to adequately describe any of the DO BTCs, as evidenced from significant deviations between modeled and experimental DO concentrations in the column outflow (Figure 5). For example, the single-reaction-kinetics model predicted complete DO breakthrough (i.e., outflow = inflow DO concentration) after approximately 24 hr (approx. 32 PV), while experimental DO outflow concentrations had not reached inflow DO concentrations at this point (Figure 5). Consequently, the single-kinetic model predicted maximum numbers of reduced POM moieties reacting with DO ($RM_{max,1}$ for single-reaction kinetics, Table 2) that were smaller than the actual equivalents of DO reduced in CBEs over 32 PV (Figure 4, Text S10 in Supporting Information S1).

Using the model with dual-reaction kinetics resulted in much better fits of the experimental BTCs, as again shown exemplarily in Figure 5 for one BTC. The good fit implies that the pool of DO reactive POM moieties had (at least) two subsets: one with fast and one with slow reaction kinetics. For all three peat soils, the fitted maximum number of slowly reacting POM moieties, $RM_{max,2}$, was approximately two-fold higher than the maximum number of fast-reacting moieties, $RM_{max,1}$ (i.e., the relative contributions of the slow to the total reacting sites were 69 ± 3% ($n = 6$) for LM, 64 ± 1% ($n = 3$) for BM and 68 ± 2% ($n = 3$)). This finding highlights the importance of reduced POM moieties that reacted only slowly with DO. The fitted reaction rate constants of the slowly reacting moieties, k_2, were approximately five-fold smaller for LM and SM, and seven-fold smaller for BM than the corresponding reaction rate constants for the fast moieties, k_1 (Table 2). The resulting reaction half-lives, $t_{1/2}$, vary between 0.15 and 0.36 hr for the fast-reacting moieties and between 0.88 and 1.91 hr for the slow-reacting moieties in POM. Reduced POM in peatland soils therefore reacts with DO over extended time scales that span from minutes up to a few hours to days.

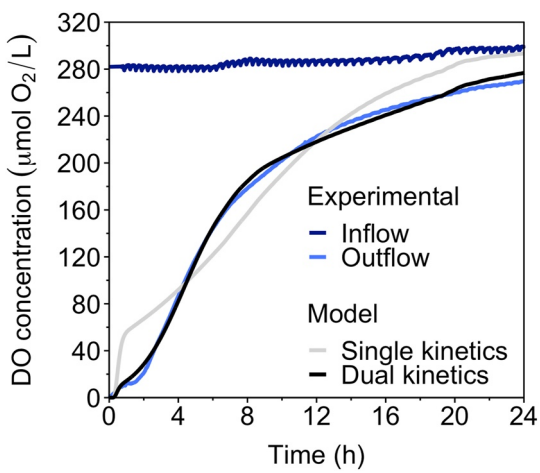

Figure 5. Dissolved oxygen (DO) breakthrough curve for a column packed with peat soil from Lungsmossen. The experimental data, replotted from Figure 2b, is fitted by the advection-dispersion transport model using either a single- or dual-kinetics terms for the reaction between DO and reduced moieties in peat particulate organic matter.

While the chemical nature of reduced POM moieties remains unidentified, it is reasonable to assume hydroquinones as candidates, given that these moieties were previously shown to dominate the redox properties of DOM (Aeschbacher et al., 2011, 2012; Klüpfel et al., 2014). While hydroquinones are oxidized to corresponding quinones by DO, this reaction is kinetically slow at low pH, particularly for quinone/hydroquinone couples with elevated standard reduction potentials (Aeschbacher et al., 2011, 2012). The slow reaction kinetics in the acidic peat soils (the pH of pore waters in LM, BM, and SM were in the range of 3.88–4.23) thus substantiate the involvement of

Table 2
Results of Model Fits to Dissolved Oxygen (DO) Breakthrough Curves (BTCs) for Columns Filled With Peat Soil From Lungsmossen (LM), Björsmossen (BM), and Storhultsmossen (SM)

	Single reaction kinetics		Dual reaction kinetics			
Location	k_1 (1/hr) $t_{1/2}$ (hr)	$RM_{max,1}$ (μmol/g POM)	k_1 (1/hr) $t_{1/2}$ (hr)	$RM_{max,1}$ (μmol/g POM)	k_2 (1/hr) $t_{1/2}$ (hr)	$RM_{max,2}$ (μmol/g POM)
LM ($n = 6$)	2.4 ± 0.3	20 ± 4	4.0 ± 0.6	8 ± 1	0.8 ± 0.2	17 ± 3
	0.29 ± 0.04		0.18 ± 0.02		0.88 ± 0.19	
BM ($n = 3$)	2.5 ± 0.4	31 ± 8	4.7 ± 1.0	14 ± 3	0.7 ± 0.2	24 ± 5
	0.28 ± 0.05		0.15 ± 0.03		1.00 ± 0.20	
SM ($n = 3$)	1.4 ± 0.5	8 ± 1	2.1 ± 0.9	3 ± 1	0.4 ± 0.1	7 ± 1
	0.52 ± 0.16		0.36 ± 0.16		1.91 ± 0.53	

Note. The fitted parameters are the maximum number of reduced moieties in peat particulate organic matter (POM) of kinetic i that react with DO ($RM_{max,i}$), reaction rate constants (k_i) (with calculated corresponding half-lives ($t_{1/2}$)) assuming either single- ($i = 1$) or dual- ($i = 1,2$) reaction kinetics for DO with reduced POM moieties in the peat soil. n is the number of experimental DO BTCs that were fitted.

hydroquinones. By contrast, re-oxidation of POM by DO is inconsistent with the suggestion that double bonds in non-reduced POM are major electron-accepting moieties (Wilson et al. (2017). Such hydrogenation of double bonds to form saturated carbon-carbon bonds cannot be reversed by DO exposure. Hydrogenation of double bonds thus cannot explain the observed DO reduction data nor how POM could act as sustained TEA over many redox cycles in peat soils.

3.2. Push-Pull Tests

We determined the kinetics and capacities of electron transfer from reduced POM to DO also in situ in the field using PPTs. These tests served to demonstrate that results from laboratory CBEs can be transferred to the field. We chose LM for these PPTs because its peat soil yielded intermediate values for $RM_{max,i}$ in CBEs among the three tested peatlands. Figure 6 shows exemplary results from the first three PPTs conducted at location LM1. These PPTs had rest periods of the injected solutions in the subsurface of ∼1.5 hr prior to re-extraction. Panel A shows the concentrations of Br^- and DO in the 15 individual solution parcels extracted from LM1, $C_{extracted}$, expressed relative to the Br^- and DO concentrations in the injected solutions, $C_{injected}$. Relative Br^- concentrations in the first extracted parcels (corresponding to injected solutions that remained closest to the injection well) were close to unity, as expected for an inert, non-reactive tracer with little dilution by peat pore water because of the proximity to the well (Figure 6a). The decrease in relative Br^- concentrations with increasing extraction parcel number reflected increased mixing of the injection solution (and thus Br^-) with the background peat pore water. A mass balance over all 15 extracted parcels showed that the cumulative amount of Br^- recovered during a PPT was equal to approximately 88% of the injected amount (Figure 6b; note that the total extracted volume was 1.5-fold larger than the injected solution volume to ensure high recoveries). As compared with Br^-, relative concentrations of DO were significantly lower in all retrieved solution parcels of the first PPT. The corresponding cumulative recovery of injected DO over all extraction parcels of the first PPT was only 28%. This finding implies that DO concentrations in the injected solution decreased not only due to mixing with subsurface peat pore water, as captured by Br^-, but also through reaction. Based on the CBE results, we consider this reaction to be the electron transfer from reduced POM to DO.

The relative DO concentrations and the cumulative DO recoveries increased from the first to second and third PPT (and in the subsequent PPTs; not shown in Figure 6b). The corresponding amounts of cumulative DO reacted in the three consecutive PPTs decreased from 54 to 29 and to 27 μmol DO, respectively (Figure 6c). This finding demonstrates continuous oxidation of reduced POM moieties with repeatedly injected DO and that this reaction consecutively lowered the number of reduced moieties that transferred electrons to DO injected in consecutive PPTs.

In each of the six wells LM1–LM6, we carried out 33 to 34 consecutive PPTs with rest periods in the subsurface varying from ∼1.5 to 23 hr (most tests had rest periods of either 1.5 hr or 18 hr). Besides co-injecting bromide

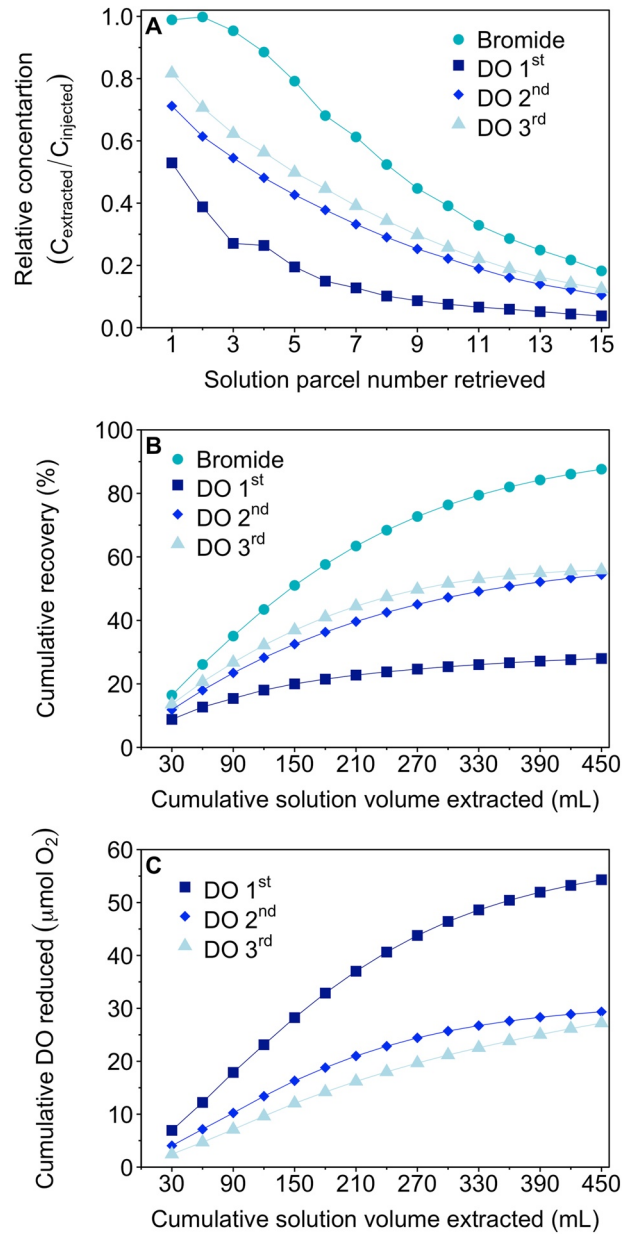

Figure 6. Results from exemplary push-pull tests (PPTs) in Lungmossen at location LM1. (a) Relative concentrations ($C_{extracetd}/C_{injected}$) of the tracer bromide (cyan circles) and dissolved oxygen (DO) in extracted solution parcels 1–15 for the first three consecutive PPTs (i.e., first, second, third), each with a ∼1.5 hr rest period of injected solutions in the subsurface. Bromide was co-injected with DO in the first PPT. (b) Cumulative recoveries over all 15 extracted solution parcels of the tracer bromide (cyan circles) and DO for each of the first three consecutive PPTs relative to the injected amounts of tracer and DO, respectively; and (c) Cumulative amounts of DO reduced in PPTs 1 to 3 over the cumulative solution volume extracted from LM1 for each test.

in the first PPT, we co-injected bromide in two additional tests over the course of the total 33 to 34 tests. These three tracer tests showed similar relative Br^- concentration profiles and Br^- recoveries for a given well (Text S12 in Supporting Information S1), demonstrating that peat physical/hydrological parameters around the wells were stable over the PPT campaign.

The cumulative amount of DO reduced at a given location steadily increased with each conducted PPT and hence with increasing cumulative amounts of injected DO (Figure 7a). Yet, the slope of the cumulative DO reduction decreased with increasing injected DO amounts, reflecting depletion of reduced POM moieties that trans-

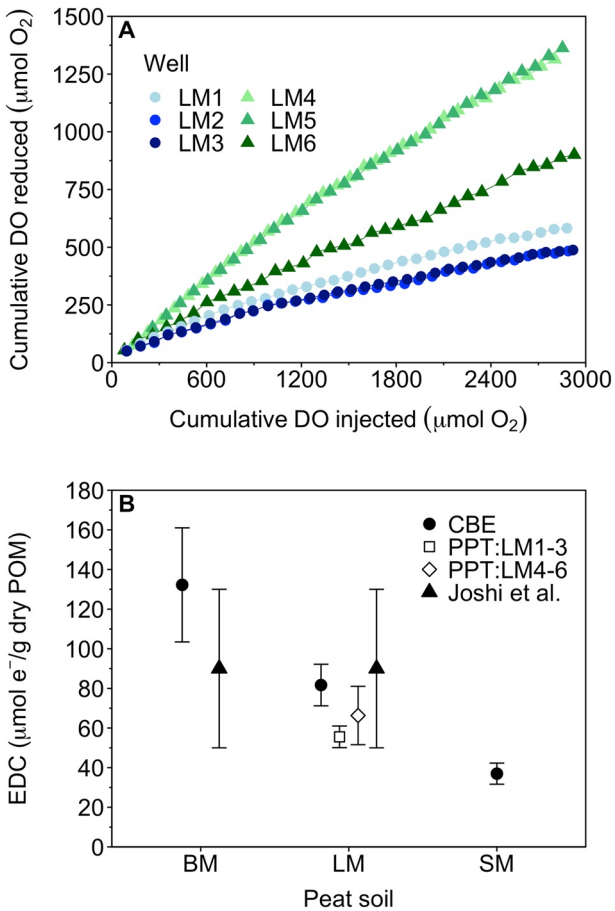

Figure 7. Results from push-pull tests (PPTs) and column breakthrough experiments (CBE) in Lungsmossen (LM) peat soil. The PPTs were conducted at two location clusters LM1–3 and LM4–6. (a) Cumulative amount of dissolved oxygen (DO) reduced plotted vs. the cumulative amount of DO injected at locations LM1 to LM6. The data points in one series corresponds to the individual consecutive 33 PPTs. (b) Electron donating capacities from peat particulate organic matter to DO calculated from decreases in DO concentrations in the PPTs in LM and, for comparison, in CBEs and in batch reoxidation experiments, reproduced from Joshi et al. (2021). The symbols and error bars correspond to averages and standard deviations, respectively ($n = 3$ in all cases except for $n = 6$ for CBEs in LM soil columns).

ferred electrons to DO and, presumably, a shift to reduced POM moieties with slower reaction kinetics with DO. In all wells, the cumulative amounts of consumed DO did not plateau over the 33 PPTs, demonstrating slow and continuous DO reduction. The cumulative DO reduced varied between locations (Figure 7a), with larger differences between the two site clusters (i.e., 14 ± 1 μmol O_2/g dry peat for cluster LM1–3 and 17 ± 4 μmol O_2/g dry peat for cluster LM4–6 (average ± standard deviation); Text S13 in Supporting Information S1). These differences likely reflected higher extents of peat-soil decomposition at the latter cluster (Text S3 in Supporting Information S1), which was supported by visual inspection of peat-soil cores retrieved from the peat after terminating the PPTs (Text S2 in Supporting Information S1).

3.3. Comparison of DO Reduction by POM in PPTs and CBEs

The calculated EDCs for LM peat soil determined in PPTs were in good agreement with the corresponding EDC values determined from CBE experiments discussed above (Figure 7b). The slightly lower EDC in PPTs than CBEs may reflect that DO consumption had not plateaued in the PPTs and, hence, that the peat soil still contained DO-reactive reduced POM moieties when we terminated the PPTs.

Figure 7b also includes the CBE-determined EDC values from BM and SM peat soil. We have previously determined the EDCs of peat POM from the same three bogs by quantifying the increase in electron-accepting capacity of the POM that resulted from exposing the in situ reduced POM to DO for 8 d (Joshi et al., 2021). The so-determined EDCs were ~90 μmol e^-/g dry POM for BM and LM (Figure 7b) and thus in good agreement with the EDCs estimated herein for these peat soils. In the previous work (Joshi et al., 2021), DO exposure of SM POM only marginally changed its electron accepting capacity, suggesting that SM was not highly reduced. Consistently, SM peat soils also showed the lowest EDC values in the CBEs conducted herein. We conclude from experiments conducted herein that POM was present in a reduced state in situ in all three tested peatlands, and that the peat POM had EDCs to DO in the range of 40–130 μmol e^-/g dry peat (including results from CBE and PPTs).

4. Conclusions

The complementary laboratory CBEs and field PPTs demonstrated that POM is present in reduced states in situ in all three tested bogs and that the reduced POM donates electrons to DO. Furthermore, for LM, CBEs and PPTs resulted in comparable numbers of electrons donated to DO per dry mass of peat soil, supporting the transferability of results from laboratory studies on reaction of POM with DO to the field. All experiments showed that DO reduction had a fast and a slow kinetic component, with reaction time scales in the range of minutes to hours and presumably up to few days. We observed variations in DO reduction by POM within a given peatland as well as by POM from different peatlands. We tentatively ascribe these differences to different extents of POM decomposition, with EDC values increasing with increasing POM decomposition degrees. The EDC values determined herein range from ~40 to 130 μmol e^-/g dry POM and are in good agreement with values previously reported for the same peat soils in laboratory POM reduction assays (Joshi et al., 2021). Furthermore, the EDC values are consistent with reported numbers of electrons transferred to POM through anaerobic microbial respiration: Keller and Takagi (2013) reported the transfer of 25 μmol e^-/g dry POM in laboratory incubation experiments performed for 30 d in the dark and without added substrates. In a different experimental setup, Gabriel et al. (2017) incubated peat-soil-filled and water-saturated microcosms and reported a transfer of ~90 μmol e^-/g dry POM after 42 d of incubation (no added substrates). Recently, Guth et al. (2022) incubated peat soil for 56 days in the dark and observed a decrease in electron-accepting capacity of ~120 μmol e^-/g dry POM.

While we did not aim to identify the chemical nature of the electron-accepting and -donating organic moieties in the POM, it is likely that quinone/hydroquinone couples play an important role, akin to their importance as redox-active moieties in DOM (Aeschbacher et al., 2011, 2012). The EDCs of 40–130 μmol e^-/g dry POM would correspond to 20–65 μmol hydroquinone groups/g dry POM, given that each hydroquinone is oxidized to the quinone by donating two electrons. With an average carbon content of 47.3% by weight in POM of our three ombrotrophic bogs (Text S3 in Supporting Information S1), and given that each hydroquinone moiety accepts two electrons and contains six carbon atoms, we can estimate between 250 and 825 μmol quinone-type aromatic carbon per g C or an aromaticity contribution of hydroquinone moieties of approximately 0.3%–1.0% of all POM carbon. This number is plausible given the values of ∼10% aromatic content reported by Tfaily et al. (2014), ∼10%–15% reported by Moody et al. (2018) and 8%–10% that we observed for POM from bogs in the Värmland county region (data not shown). These calculations in combination with electron transfer reversibility determined herein support that quinone moieties, not aliphatic double bonds (see above), are involved in POM acting as TEA.

The finding of reduced POM under anoxic conditions in situ and its re-oxidation by DO substantiates not only that POM acts as TEA in anerobic microbial respiration under anoxic conditions, but also that the capacity of POM to accept electrons can be restored through oxidation by DO entering the peat soil during recurring oxygenation events, for example, through water-table drawdowns, strong water-infiltration events, and through the release of photosynthetically formed O_2 through roots or rhizoids (Björn et al., 2022). This re-oxidation is a pre-requisite for POM to act as a regenerable, long-term TEA near the oxic-anoxic interface in peatlands.

Assuming that the herein reported EDCs of POM resulted from its reduction as TEA in anaerobic respiration, we can estimate the extent to which anaerobic respiration to POM may lower methane concentrations (or mass) per unit area in peatlands, either through competitive suppression of methanogenesis or by AOM. For a unit area of 1 km^2 we assumed an average yearly water-table fluctuation of 25 cm (Fraser et al., 2001; Treat et al., 2007). Using our measured peat dry-bulk densities of 56–86 g/L (Text S9 in Supporting Information S1), we computed a peat dry mass of 130–200 Tg per km^2 of peatland that could act as TEA in anaerobic respiration. This peat mass would allow for an electron transfer of $7.3 \pm 0.7 \times 10^5$ to $1.3 \pm 0.3 \times 10^6$ mol e^- km^{-2} yr^{-1}. For the oxidation of 1 mol CH_4 to CO_2 in AOM, 8 mol e^- need to be transferred. Likewise, to suppress the production of 1 mol CH_4 by allowing for anaerobic respiration instead of methanogenesis requires the transfer of 8 mol e^- to POM when respiring a substrate with an assumed nominal oxidation state of carbon of zero. This means that re-oxidation of reduced POM in the peat-soil layer affected by water-table fluctuations may lower the amount of CH_4 in the studied peatlands by $9.1 \pm 0.9 \times 10^4$ to $1.6 \pm 0.4 \times 10^5$ mol CH_4 km^{-2} yr^{-1}. This potential decrease in the CH_4 amount is significant when compared with the reported emissions of $1–18 \times 10^5$ mol CH_4 km^{-2} yr^{-1} for northern peatlands (Blodau, 2002), and estimated emissions of 43×10^5 mol CH_4 km^{-2} yr^{-1} for peatlands globally (Guth et al., 2022).

Data Availability Statement

The datasets required to analyze the results and replicate the research from this manuscript are provided as supplementary information and separate .csv files. These will be published at the ETH Research Collection webpage (https://doi.org/10.3929/ethz-b-000635112; Obradović et al., 2023). For the use of Aquasim 2.0 software (Reichert, 1994, 1998), the open-access package is available via the link https://www.eawag.ch/en/department/siam/software/, under the tab "AQUASIM". Data analyses and plotting were performed in open-access software RStudio (Posit team, 2022; Signorell et al., 2017; Wickham, 2016; Wickham & Bryan, 2023; Wickham et al., 2019, 2023; Wilke, 2020).

Acknowledgments
We thank Klaus-Holger Knorr (Westfälische Wilhelms-Universität Münster, Germany) for his help during the field work, as well as Stefan Meier (ETH Zürich, Switzerland) for his help in building the samplers for field experiments. We also thank two anonymous reviewers for their valuable suggestions. Prachi Joshi (now Eberhard Karls Universität Tübingen, Germany) acknowledges funding from ETH Postdoctoral Fellowship Program (Grant ETH/COFUND 18-1 FEL-34). Michael Sander and Martin H. Schroth (ETH Zürich, Switzerland) acknowledge funding from the Swiss National Science Foundation (SNSF; Project number 200020_182645). Open Access Funding provided by Eidgenossische Technische Hochschule Zürich.

References

Aeschbacher, M., Schwarzenbach, R. P., & Sander, M. (2012). Antioxidant properties of humic substances. *Environmental Science & Technology*, *46*(9), 4916–4925. https://doi.org/10.1021/es300039h

Aeschbacher, M., Vergari, D., Schwarzenbach, R. P., & Sander, M. (2011). Electrochemical analysis of proton and electron transfer equilibria of the reducible moieties in humic acids. *Environmental Science & Technology*, *45*(19), 8385–8394. https://doi.org/10.1021/es201981g

Agethen, S., Sander, M., Waldemer, C., & Knorr, K.-H. (2018). Plant rhizosphere oxidation reduces methane production and emission in rewetted peatlands. *Soil Biology and Biochemistry*, *125*, 125–135. https://doi.org/10.1016/j.soilbio.2018.07.006

Almquist-Jacobson, H., & Foster, D. R. (1995). Toward an integrated model for raised-bog development: Theory and field evidence. *Ecology*, *76*(8), 2503–2516. https://doi.org/10.2307/2265824

Amaral, J. A., & Knowles, R. (1994). Methane metabolism in a temperate swamp. *Applied and Environmental Microbiology*, *60*(11), 3945–3951. https://doi.org/10.1128/aem.60.11.3945-3951.1994

Beer, J., Lee, K., Whiticar, M., & Blodau, C. (2008). Geochemical controls on anaerobic organic matter decomposition in a northern peatland. *Limnology & Oceanography*, *53*(4), 1393–1407. https://doi.org/10.4319/lo.2008.53.4.1393

Björn, L. O., Middleton, B. A., Germ, M., & Gaberščik, A. (2022). Ventilation systems in wetland plant species. *Diversity*, *14*(7), 517–538. https://doi.org/10.3390/d14070517

Blodau, C. (2002). Carbon cycling in peatlands—A review of processes and controls. *Environmental Reviews*, *10*(2), 111–134. https://doi.org/10.1139/a02-004

Bridgham, S. D., Cadillo-Quiroz, H., Keller, J. K., & Zhuang, Q. (2013). Methane emissions from wetlands: Biogeochemical, microbial and modelling perspectives from local to global scales. *Global Change Biology*, *19*(5), 1325–1346. https://doi.org/10.1111/gcb.12131

Broder, T., Blodau, C., Biester, H., & Knorr, K.-H. (2012). Peat decomposition records in three pristine ombrotrophic bogs in southern Patagonia. *Biogeosciences*, *9*(4), 1479–1491. https://doi.org/10.5194/bg-9-1479-2012

Christensen, T. R., Michelsen, A., Jonasson, S., & Schmidt, I. K. (1997). Carbon dioxide and methane exchange of a subarctic heath in response to climate change related environmental manipulations. *Oikos*, *79*(1), 34–44. https://doi.org/10.2307/3546087

Efremenko, E., Senko, O., Stepanov, N., Mareev, N., Volikov, A., & Perminova, I. (2020). Suppression of methane generation during methanogenesis by chemically modified humic compounds. *Antioxidants*, *9*(11), 1140. https://doi.org/10.3390/antiox9111140

Estop-Aragones, C., Knorr, K.-H., & Blodau, C. (2012). Controls on in situ oxygen and dissolved inorganic carbon dynamics in peats of a temperate fen. *Journal of Geophysical Research*, *117*(52), 1–14. https://doi.org/10.1029/2011JG001888

Forster, P., Ramaswamy, V., Artaxo, P., Berntsen, T., Betts, R., Fahey, D. W., et al. (2007). Climate change 2007. In S. Solomon (Ed.), *The physical science basis* (pp. 131–234).

Fraser, C. J. D., Roulet, N. T., & Moore, T. R. (2001). Hydrology and dissolved organic carbon biogeochemistry in an ombrotrophic bog. *Hydrology*, *15*(16), 3151–3166. https://doi.org/10.1002/hyp.322

Freeman, C., Ostle, N., & Kang, H. (2001). An enzymic 'latch' on a global carbon store. *Nature*, *409*(6817), 149. https://doi.org/10.1038/35051650

Gabriel, K. N., Medvedeff, C. A., & Keller, J. K. (2017). Microbial organic matter reduction in a peatland soil: The importance of water-table level. *BIOS*, *88*(1), 39–45. https://doi.org/10.1893/BIOS-D-16-00002.1

Gao, C., Sander, M., Agethen, S., & Knorr, K.-H. (2019). Electron accepting capacity of dissolved and particulate organic matter control CO_2 and CH_4 formation in peat soils. *Geochimica et Cosmochimica Acta*, *245*, 266–277. https://doi.org/10.1016/j.gca.2018.11.004

Gorecki, K., Rastogi, A., Strozecki, M., Gabka, M., Lamentowicz, M., Lucow, D., et al. (2021). Water table depth, experimental warming, and reduced precipitation impact on litter decomposition in a temperate Sphagnum-peatland. *Science of the Total Environment*, *771*, 145452. https://doi.org/10.1016/j.scitotenv.2021.145452

Gorham, E. (1991). Northern peatlands: Role in the carbon cycle and probable responses to climatic warming. *Ecological Applications*, *1*(2), 182–195. https://doi.org/10.2307/1941811

Guth, P., Gao, C., & Knorr, K.-H. (2022). Electron accepting capacities of a wide variety of peat materials from around the globe similarly explain CO_2 and CH_4 formation. *Journal of Geophysical Research: Biogeosciences*, *37*, 1–20. https://doi.org/10.1029/2022GB007459

Heitmann, T., Goldhammer, T., Beer, J., & Blodau, C. (2007). Electron transfer of dissolved organic matter and its potential significance for anaerobic respiration in a northern bog. *Global Change Biology*, *13*(8), 1771–1785. https://doi.org/10.1111/j.1365-2486.2007.01382.x

Hiederer, R., & Köchy, M. (2011). *Global soil organic carbon estimates and the harmonized world soil database* (p. 79). EUR 25225 EN. Publications Office of the European Union.

IPCC. (2022). Climate change 2022: Mitigation of climate change. In P. R. Shukla, J. Skea, R. Slade, A. Al Khourdajie, R. van Diemen, D. McCollum, et al. (Eds.), *Contribution of working group III to the sixth assessment report of the intergovernmental panel on climate change*. Cambridge University Press. https://doi.org/10.1017/9781009157926

Joshi, P., Schroth, M. H., & Sander, M. (2021). Redox properties of peat particulate organic matter: Quantification of electron accepting capacities and assessment of electron transfer reversibility. *Journal of Geophysical Research: Biogeosciences*, *126*(8), 1–18. https://doi.org/10.1029/2021JG006329

Keller, J. K., & Takagi, K. K. (2013). Solid-phase organic matter reduction regulates anaerobic decomposition in bog soil. *Ecosphere*, *4*(5), 1–12. https://doi.org/10.1890/ES12-00382.1

Keller, J. K., Weisenhorn, P. B., & Megonigal, J. P. (2009). Humic acids as electron acceptors in wetland decomposition. *Soil Biology and Biochemistry*, *41*(7), 1518–1522. https://doi.org/10.1016/j.soilbio.2009.04.008

Klüpfel, L., Piepenbrock, A., Kappler, A., & Sander, M. (2014). Humic substances as fully regenerable electron acceptors in recurrently anoxic environments. *Nature Geoscience*, *7*(3), 195–200. https://doi.org/10.1038/ngeo2084

Lai, D. Y. F. (2009). Methane dynamics in northern peatlands: A review. *Pedosphere*, *19*(4), 409–421. https://doi.org/10.1016/S1002-0160(09)00003-4

Lindsay, R. (2016). Peatland (mire types): Based on origin and behavior of water, peat genesis, landscape position, and climate. In C. Finlayson, G. Milton, R. Prentice, & N. Davidson (Eds.), *The wetland book*. Springer. https://doi.org/10.1007/978-94-007-6173-5_279-1

Lovley, D. R., Coates, J. D., Blunt-Harris, E. L., Phillips, E. J. P., & Woodward, J. C. (1996). Humic substances as electron acceptors for microbial respiration. *Nature*, *382*(6590), 445–448. https://doi.org/10.1038/382445a0

Lovley, D. R., Fraga, J. L., Blunt-Harris, E. L., Hayes, L. A., Phillips, E. J. P., & Coates, J. D. (1998). Humic substances as a mediator for microbially catalyzed metal reduction. *Acta Hydrochimica et Hydrobiologica*, *26*(3), 152–157. https://doi.org/10.1002/(SICI)1521-401X(199805)26:3<152::AID-AHEH152>3.0.CO;2-D

Moody, C. S., Worral, F., Clay, G. D., Burt, T. P., Apperley, D. C., & Rose, R. (2018). A molecular budget for a peatland based upon ^{13}C solid-state nuclear magnetic resonance. *Journal of Geophysical Research: Biogeosciences*, *123*(2), 547–560. https://doi.org/10.1002/2017JG004312

Moore, T., Blodau, C., Turunen, J., Roulet, N., & Richard, P. J. H. (2005). Patterns of nitrogen and sulfur accumulation and retention in ombrotrophic bogs, eastern Canada. *Global Change Biology*, *11*(2), 356–367. https://doi.org/10.1111/j.1365-2486.2004.00882.x

Nichols, J. E., & Peteet, D. M. (2019). Rapid expansion of northern peatlands and doubled estimate of carbon storage. *Nature Geoscience*, *12*(11), 917–921. https://doi.org/10.1038/s41561-019-0454-z

Obradović, N., Joshi, P., Arn, S., Aeppli, M., Schroth, M. H., & Sander, M. (2023). Reoxidation of reduced peat organic matter by dissolved oxygen: Combined laboratory and column-breakthrough experiments and in-field push-pull tests [Dataset]. Journal of Geophysical Research: Biogeosciences, *126*, 8. https://doi.org/10.1029/2021jg006329

Posit team. (2022). RStudio: Integrated development environment for R [Software]. Posit Software, BC, Boston, MA. (Version 2022.12.0.353, USA). Retrieved from http://www.posit.co/

Ralston, M. L., & Jennrich, R. I. (1978). Dud, a derivative-free algorithm for nonlinear least squares. *Technometrics*, *20*(1), 7–14. https://doi.org/10.1080/00401706.1978.10489610

Reichert, P. (1994). AQUASIM—A tool for simulation and data analysis of aquatic systems [Software]. Water Science and Techology, *30*(2), 21–30. https://doi.org/10.2166/wst.1994.0025

Reichert, P. (1998). AQUASIM 2.0—User manual [Dataset]. Swiss Federal Institute for Environmental Science and Technology (EAWAG). Retrieved from https://www.eawag.ch/en/department/siam/software/

Rissanen, A. J., Karvinen, A., Nykänen, H., Peura, S., Tiirola, M., Mäki, A., & Kankaala, P. (2017). Effects of alternative electron acceptors on the activity and community structure of methane-producing and consuming microbes in the sediments of two shallow boreal lakes. *FEMS Microbiology Ecology*, *93*(7), 1–16. https://doi.org/10.1093/femsec/fix078

Roden, E. E., Kappler, A., Bauer, I., Jiang, J., Paul, A., Stoesser, R., et al. (2010). Extracellular electron transfer through microbial reduction of solid-phase humic substances. *Nature Geoscience*, *3*(6), 417–421. https://doi.org/10.1038/ngeo870

Rydin, H., & Jeglum, J. (2013). The biology of peatlands (2nd ed.). https://doi.org/10.1111/aec.12290

Salmon, E., Jégou, F., Guenet, B., Jourdain, L., Qiu, C., Bastrikov, V., et al. (2022). Assessing methane emissions for northern peatlands in ORCHIDEE-PEAT revision 7020. *Geoscientific Model Development*, *15*(7), 2813–2838. https://doi.org/10.5194/gmd-15-2813-2022

Saunois, M., Stavert, A. R., Poulter, B., Bousquet, P., Canadell, J. G., Jackson, R. B., et al. (2020). The global methane budget 2000–2017. *Earth System Science Data*, *12*(3), 1561–1623. https://doi.org/10.5194/essd-12-1561-2020

Scharlemann, J. P. W., Tanner, E. V. J., Hiederer, R., & Kapos, V. (2014). Global soil carbon: Understanding and managing the largest terrestrial carbon pool. *Carbon Management*, *5*(1), 81–91. https://doi.org/10.4155/cmt.13.77

Scheffer, R. A., van Logtestijn, R. S. P., & Verhoeven, J. T. A. (2001). Decomposition of Carex and sphagnum litter in two mesotrophic fens differing in dominant plant species. *Oikos*, *92*(1), 44–54. https://doi.org/10.1034/j.1600-0706.2001.920106.x

Scheller, S., Yu, H., Chadwick, G. L., McGlynn, S. E., & Orphan, V. J. (2016). Artificial electron acceptors decouple archaeal methane oxidation from sulfate reduction. *Science*, *351*(6274), 703–707. https://doi.org/10.1126/science.aad7154

Scott, D. T., McKnight, D. M., Blunt-Harris, E. L., Kolesar, S. E., & Lovley, D. R. (1998). Quinone moieties act as electron acceptors in the reduction of humic substances by humics-reducing microorganisms. *Environmental Science & Technology*, *32*(19), 2984–2989. https://doi.org/10.1021/es980272q

Segers, R., & Kengen, S. W. M. (1998). Methane production as a function of anaerobic carbon mineralization: A process model. *Soil Biology and Biochemistry*, *30*(8), 1107–1117. https://doi.org/10.1016/S0038-0717(97)00198-3

Signorell, A., Aho, K., Alfons, A., et al. (2017). DescTools: Tools for descriptive statistics [Software]. R package version 0.99.23. Retrieved from https://github.com/AndriSignorell/DescTools/

Smemo, K. A., & Yavitt, J. B. (2007). Evidence for anaerobic CH 4 oxidation in freshwater peatlands. *Geomicrobiology Journal*, *24*(7–8), 583–597. https://doi.org/10.1080/01490450701672083

Smemo, K. A., & Yavitt, J. B. (2011). Anaerobic oxidation of methane: An underappreciated aspect of methane cycling in peatland ecosystems? *Biogeosciences*, *8*(3), 779–793. https://doi.org/10.5194/bg-8-779-2011

Stepniewski, W., & Glinski, J. (1988). Gas exchange and atmospheric properties of flooded soils. In *The ecology and management of wetlands*. Springer. https://doi.org/10.1007/978-1-4684-8378-9_23

Tfaily, M. M., Cooper, W. T., Kostka, J. E., Chanton, P. R., Schadt, C. W., Hanson, P. J., et al. (2014). Organic matter transformation in the peat column at Marcell Experimental Forest: Humification and vertical strati-fication. *Journal of Geophysical Research: Biogeosciences*, *119*(4), 661–675. https://doi.org/10.1002/2013JG002492

Treat, C. C., Bubier, J. L., Varner, R. K., & Crill, P. M. (2007). Timescale dependence of environmental and plant-mediated controls on CH_4 flux in a temperate fen. *Journal of Geophysical Research*, *112*(G1), G01014. https://doi.org/10.1029/2006JG000210

Tuominen, L., Kairesalo, T., & Hartikainen, H. (1994). Comparison of methods for inhibiting bacterial activity in sediment. *Applied and Environmental Microbiology*, *60*(9), 3454–3457. https://doi.org/10.1128/aem.60.9.3454-3457.1994

Walpen, N., Getzinger, G. J., Schroth, M. H., & Sander, M. (2018a). Electron-Donating phenolic and electron-accepting quinone moieties in peat dissolved organic matter: Quantities and redox transformations in the context of peat biogeochemistry. *Environmental Science & Technology*, *52*(9), 5236–5245. https://doi.org/10.1021/acs.est.8b00594

Walpen, N., Lau, M. P., Fiskal, A., Getzinger, G. J., Meyer, S. A., Nelson, T. F., et al. (2018b). Oxidation of reduced peat particulate organic matter by dissolved oxygen: Quantification of apparent rate constants in the field. *Environmental Science & Technology*, *52*(19), 11151–11160. https://doi.org/10.1021/acs.est.8b03419

Walpen, N., Schroth, M. H., & Sander, M. (2016). Quantification of phenolic antioxidant moieties in dissolved organic matter by flow-injection analysis with electrochemical detection. *Environmental Science & Technology*, *50*(12), 6423–6432. https://doi.org/10.1021/acs.est.6b01120

Wickham, H. (2016). ggplot2: Elegant graphics for data analysis [Software]. Springer-Verlag. Retrieved from https://ggplot2.tidyverse.org

Wickham, H., Averick, M., Bryan, J., Chang, W., McGowan, L. D., François, R., et al. (2019). Welcome to the tidyverse [Software]. Journal of Open Source Software, *4*(43), 1686. https://doi.org/10.21105/joss.01686

Wickham, H., & Bryan, J. (2023). readxl: Read excel files [Software]. GitHub. Retrieved from https://github.com/tidyverse/readxl

Wickham, H., François, R., Henry, L., Müller, K., & Vaughan, D. (2023). dplyr: A grammar of data manipulation [Software]. GitHub. Retrieved from https://github.com/tidyverse/dplyr

Wilke, C. (2020). cowplot: Streamlined plot theme and plot annotations for 'ggplot2' [Software]. R package version 1.1.1. Retrieved from https://CRAN.R-project.org/package=cowplot

Wilson, R. M., Tfaily, M. M., Rich, V. I., Keller, J. K., Bridgham, S. D., Zalman, C. M., et al. (2017). Hydrogenation of organic matter as terminal electron sink sustains high CO_2:CH_4 production ratios during anaerobic decomposition. *Organic Geochemistry*, *112*, 22–32. https://doi.org/10.1016/j.orggeochem.2017.06.011

Yang, W. H., McNicol, G., Teh, Y. A., Estera-Molina, K., Wood, T. E., & Silver, W. L. (2017). Evaluating the classical versus an emerging conceptual model of peatland methane dynamics. *Global Biogeochemical Cycles*, *31*(9), 1435–1453. https://doi.org/10.1002/2017GB005622

Ye, R., Keller, J. K., Jin, Q., Bohannan, B. J. M., & Bridgham, S. D. (2016). Peatland types influence the inhibitory effects of a humic substance analog on methane production. *Geoderma*, *265*, 131–140. https://doi.org/10.1016/j.geoderma.2015.11.026

Yu, Z., Beilman, D. W., Frolking, S., MacDonald, G. M., Roulet, N. T., Camill, P., & Charman, D. J. (2011). Peatlands and their role in the global carbon cycle. *Eos Trans. AGU*, *92*(12), 97–98. https://doi.org/10.1029/2011EO120001

Yu, Z. C. (2012). Northern peatland carbon stocks and dynamics: A review. *Biogeosciences*, *9*(10), 4071–4085. https://doi.org/10.5194/bg-9-4071-2012

Yu, Z.-G., Göttlicher, J., Steininger, R., & Knorr, K.-H. (2016). Organic sulfur and organic matter redox processes contribute to electron flow in anoxic incubations of peat. *Environmental Chemistry*, *13*(5), 816–825. https://doi.org/10.1071/en15091

References From the Supporting Information

Barsch, D., Fierz, H., & Haeberli, W. (1979). Shallow core drilling and bore-hole measurements in the permafrost of an active rock glacier near the Grubengletscher, Wallis, Swiss Alps. *Arctic and Alpine Research*, *11*(2), 215–228. https://doi.org/10.2307/1550646

Clymo, R. S. (1963). Ion exchange in sphagnum and its relation to bog ecology. *Annals of Botany*, *27*(106), 309–324. https://doi.org/10.1093/oxfordjournals.aob.a083847

Franchini, A. G., & Zeyer, J. (2012). Freeze-coring method for characterization of microbial community structure and function in wetland soils at high spatial resolution. *Applied and Environmental Microbiology*, *78*(9), 4501–4504. https://doi.org/10.1128/AEM.00133-12

Hájek, T., Ballance, S., Limpens, J., Zijlstra, M., & Verhoeven, J. T. A. (2011). Cell-wall polysaccharides play an important role in decay resistance of *Sphagnum* and actively depressed decomposition in vitro. *Biogeochemistry*, *103*(1–3), 45–57. https://doi.org/10.1007/s10533-010-9444-3

Leifeld, J., Klein, K., & Wüst-Galley, C. (2020). Soil organic matter stoichiometry as indicator for peatland degradation. *Scientific Reports*, *10*(1), 7634–7642. https://doi.org/10.1038/s41598-020-64275-y

Nauer, P. A., & Schroth, M. H. (2010). In situ quantification of atmospheric methane oxidation in near-surface soils. *Vadose Zone Journal*, *9*(4), 1052–1062. https://doi.org/10.2136/vzj2009.0192

Serk, H., Nilsson, M. B., Figueira, J., Krüger, J. P., Leifeld, J., Alewell, C., & Schleucher, J. (2022). Organochemical characterization of peat reveals decomposition of specific hemicellulose structures as the main cause of organic matter loss in the acrotelm. *Environmental Science & Technology*, *56*(23), 17410–17419. https://doi.org/10.1021/acs.est.2c03513

Teickner, H., Gao, C., & Knorr, K.-H. (2022). Electrochemical properties of peat particulate organic matter on a global scale: Relation to peat chemistry and degree of decomposition. *Global Biogeochemical Cycles*, *36*(2), e2021GB007160. https://doi.org/10.1029/2021GB007160

Thomas, P. A., & Pearce, D. M. E. (2004). Role of cation exchange in preventing the decay of anoxic deep bog peat. *Soil Biology and Biochemistry*, *36*(1), 23–32. https://doi.org/10.1016/j.soilbio.2003.07.003

Verhoeven, J. T. A., & Liefveld, W. M. (1997). The ecological significance of organochemical compounds in Sphagnum. *Acta Botanica Neerlandica*, *46*(2), 117–130. https://doi.org/10.1111/plb.1997.46.2.117

Wang, M., Moore, T. R., Talbot, J., & Riley, J. L. (2015). The stoichiometry of carbon and nutrients in peat formation. *Global Biogeochemical Cycles*, *29*(2), 113–121. https://doi.org/10.1002/2014gb005000

Whittington, P., Koiter, A., Watts, D., Brewer, A., & Golubev, V. (2021). Bulk density, particle density, and porosity of two species of *Sphagnum*: Variability in measurement techniques and spatial distribution. *Soil Science Society of America Journal*, *85*(6), 2220–2233. https://doi.org/10.1002/saj2.20327